

Document downloaded from:

<http://hdl.handle.net/10251/150361>

This paper must be cited as:

Page Del Pozo, AF.; De Rosario Martínez, H.; Galvez Griso, JA.; Mata Amela, V. (2011). Representation of planar motion of complex joints by means of rolling pairs. Application to neck motion. *Journal of Biomechanics*. 44(4):747-750.
<https://doi.org/10.1016/j.jbiomech.2010.11.019>



The final publication is available at

<https://doi.org/10.1016/j.jbiomech.2010.11.019>

Copyright ELSEVIER SCI LTD

Additional Information

Manuscript Type: Short Communication

Representation of planar motion of complex joints by means of rolling pairs.

Application to neck motion.

Álvaro Page^{a,b}, Helios de Rosario^c, José A. Gálvez^c, Vicente Mata^d

Corresponding author: Álvaro Page
Departamento de Física Aplicada
Universidad Politécnica de Valencia
Camino de Vera, s/n
E46022 VALENCIA (Spain)
afpage@ibv.upv.es
Phone: +34963879160; fax: +34963879169

^aDepartamento de Física Aplicada. Universidad Politécnica de Valencia

^bCIBER de Bioingeniería, Biomateriales y Nanomedicina (CIBER-BBN)

^cInstituto de Biomecánica de Valencia. Universidad Politécnica de Valencia

^dDepartamento de Ingeniería Mecánica. Universidad Politécnica de Valencia

Keywords

Kinematic analysis
Human movement
Stereophotogrammetry
Instantaneous helical axis
Motion modeling

Word count: 1571 words

1 **Short Communication**

2 **Representation of planar motion of complex joints by means of rolling pairs.**

3 **Application to neck motion.**

4 **Abstract**

5 We propose to model planar movements between two human segments by means of
6 rolling-without-slipping kinematic pairs. We compute the path traced by the instantaneous
7 center of rotation (ICR) as seen from the proximal and distal segments, thus obtaining the
8 fixed and moving centrodes, respectively. The joint motion is then represented by the
9 rolling-without-slipping of one centrode on the other. The resulting joint kinematic model is
10 based on the real movement and accounts for nonfixed axes of rotation; therefore it could
11 improve current models based on revolute pairs in those cases where joint movement
12 implies displacement of the ICR. Previous authors have used the ICR to characterize human
13 joint motion, but they only considered the fixed centrode. Such an approach is not adequate
14 for reproducing motion because the fixed centrode by itself does not convey information
15 about body position. The combination of the fixed and moving centrodes gathers the
16 kinematic information needed to reproduce the position and velocities of moving bodies. To
17 illustrate our method, we applied it to the flexion-extension movement of the head relative
18 to the thorax. The model provides a good estimation of motion both for position variables
19 (mean $R_{\text{pos}}=0.995$) and for velocities (mean $R_{\text{vel}}=0.958$). This approach is more realistic
20 than other models of neck motion based on revolute pairs, such as the dual-pivot model. The
21 geometry of the centrodes can provide some information about the nature of the movement.
22 For instance, the ascending and descending curve of the fixed centrode suggests a
23 sequential movement of the cervical vertebrae.

24

25 **1. Introduction**

26 The modeling of human motion is relevant for its applications in clinical and
27 ergonomic fields. In whole-body models, even complex joints such as the lumbar spine,
28 shoulder complex or neck are usually simplified to just one or two lower pairs whose axes
29 pass through a fixed point (Goossens and Snijders, 1995; Petuskey et al., 2007; Willinger,
30 2005). However, several studies have shown that complex joints have a moving axis of
31 rotation even in simple motions, such as flexion-extension (Woltring et al., 1994, Page et
32 al., 2009a, Page et al., 2010). This limitation can be avoided by modeling complex
33 articulations with a higher number of lower pairs (Van der Helm et al., 1992), or including
34 all vertebrae as segments of the model (Himmeloglu et al., 2007; de Zee et al. 2008). Such
35 models improve realism at the expense of introducing kinematic redundancy and
36 complexity, which limits their usefulness for clinical routine or ergonomic applications.

37 A different approach uses the instantaneous helical axis (IHA) to characterize joint
38 movements (Leardini et al., 1999; Wolf and Degani 2007; Grip et al., 2008). Nevertheless,
39 the IHA does not actually provide a joint model because the IHA by itself does not
40 represent relative position and orientation. These features need to be evaluated by a separate
41 finite displacement analysis. The equivalent of the IHA in planar motion is the
42 instantaneous center of rotation (ICR).

43 In this paper, we use both finite and instantaneous displacements to provide a
44 geometrical model of planar motions. This model is obtained as a higher kinematic pair
45 constituted by the proximal and distal centrodes as the one rolls without slipping on the
46 other (Reuleaux, 1876), thus being compatible with a nonfixed ICR. The fixed and moving
47 centrodes are the curves traced by the ICR as seen from the proximal and distal segments,
48 respectively.

49 The rolling-without-slipping pair (subsequently called “rolling pair”) is a one
 50 degree-of-freedom (DOF) model. The theoretical basis for modeling a complex joint as a
 51 one-DOF pair is provided by the concept of functional DOFs (fDOF) (Li, 2006). A human
 52 movement is said to have one fDOF when all degrees of freedom are coordinated such that
 53 all the kinematic variables can be expressed as functions of only one independent DOF.

54 The model is illustrated with an experimental study of neck flexion-extension
 55 movement. We tested the goodness of the rolling pair model and compared it with a model
 56 based on two revolute pairs (Woltring et al., 1994).

57 **2. Methods**

58 *2.1. Kinematic model*

59 A planar motion can have up to three DOFs: a rotation angle, θ , and the two
 60 components of the displacement of a given point G , $\Delta\mathbf{R}_G$, on the plane of motion.
 61 However, natural movements are coordinated, so these variables do not vary independently.
 62 In the theoretical case that the condition of having one fDOF is satisfied, it is possible to
 63 express the kinematic variables as a function of the joint angle $\theta(t)$ and its time derivative
 64 $\dot{\theta}(t)$ (Page et al., 2010):

$$65 \quad \Delta\mathbf{R}_G = \Delta\mathbf{R}_G(\theta) \quad (1)$$

$$66 \quad \mathbf{w} = \dot{\theta} \mathbf{u} = \mathbf{w} \mathbf{u} \quad (2)$$

$$67 \quad \mathbf{v}_G = \frac{d\mathbf{R}_G}{d\theta} \dot{\theta} = \mathbf{v}_s(\theta) \mathbf{w} \quad (3)$$

68 where \mathbf{w} and \mathbf{v}_G are the angular and linear velocities respectively, \mathbf{u} is the unit
 69 vector perpendicular to the plane of motion and \mathbf{v}_s is a standardized velocity representing

70 the displacement of G per unit of joint rotation. The location of ICR, H is given by (Figure
71 1a):

$$72 \quad \mathbf{GH}(\theta) = \frac{\mathbf{w} \times \mathbf{v}_G}{w^2} = \frac{\dot{\theta} \mathbf{u} \times \dot{\theta} \mathbf{v}_S}{\dot{\theta}^2} = \mathbf{u} \times \mathbf{v}_S(\theta) \quad (4)$$

73 As the motion occurs, point H traces a planar curve called the fixed centrode. The
74 moving centrode is the curve traced by the ICR of the relative motion of the proximal
75 segment as seen from the distal one, H_1 . This curve can be computed by applying the finite
76 displacement $\{-\theta \mathbf{u}, -\Delta \mathbf{R}_G\}$ to the distal body at the current position (Figure 1b). Point H
77 therefore moves “backwards” to H_1 (Page et al 2009b):

$$78 \quad \mathbf{HH}_1 = -\Delta \mathbf{R}_G - \sin \theta \mathbf{u} \times \mathbf{GH} + (1 - \cos \theta) \mathbf{u} \times (\mathbf{u} \times \mathbf{GH}) \quad (5)$$

79 The movement can be reproduced exactly as the rolling-without-slipping motion of
80 the moving centrode on the fixed one.

81 In practice, the relation between $\Delta \mathbf{R}_G$ and θ is not completely single-valued due to
82 variability across repetitions of the same motion. For this reason, it is necessary to obtain an
83 average motion that represents the typical motion performed by a subject when repeating
84 the same movement a number of times (Page et al., 2010). The rolling pair is thus obtained
85 from this averaged movement.

86 2.2. Experiment

87 The model has been applied to the neck flexion-extension movement in order to
88 illustrate its usefulness. Twelve healthy volunteers participated in the study (6 male, 6
89 female) aged between 25 and 65 (mean=43.6 years old, SD=13.3 years old). All subjects
90 signed an informed consent form.

91 Subjects sat on a chair with their back upright and firmly held against the backrest
92 by means of straps (Baydal-Bertomeu et al., 2007). Each subject performed several cycles
93 of flexion-extension at a self-selected speed for 30s, starting from a neutral posture.

94 Head position and movements were recorded using stereophotogrammetry
95 (Kinescan©, Page et al., 2009b) with passive markers fixed onto a helmet. Three additional
96 markers were placed in the ears and at the C7 apophysis in order to have anatomical
97 references.

98 A 3D kinematic analysis was performed by using the procedures described in Page
99 et al. (2009b). From these 3D variables we checked the hypothesis of one fDOF and planar
100 motion and then computed the centrodes that represented the averaged movement across
101 cycles (Page et al., 2010). The centrodes were computed from this averaged movement.

102 The rolling pair model was compared with the dual pivot model, which represents
103 the neck joint by means of two revolute pairs, one at the level of the center of C7-T1 and
104 the other at the C1 level (Woltring et al. 1994). The instantaneous values of joint angles
105 were computed from photogrammetric measures.

106 **3. Results**

107 Table 1 summarizes the results of the experiment. The adjustment between
108 measured and fitted kinematic variables is good ($R_{\text{pos}} = 0.995$; $R_{\text{vel}} = 0.958$). The results
109 confirm the hypothesis of a single fDOF.

110 With regard to the planar motion hypothesis, the deviation between $\mathbf{w}(t)$ and \mathbf{u} was
111 small in all subjects ($p95(\alpha) = 3.9^\circ$). Moreover, linear and angular velocities were
112 perpendicular throughout the range of movement in all cases ($p95(\beta) = 2.1^\circ$).

113 Fig. 2 shows the centrodes for a subject, plotted at the reference posture. This
114 picture is animated in the electronic version in order to show the field of standardized
115 velocities at each position.

116 Fig. 3 shows the trajectories of anatomical point O (the midpoint of markers located
117 at ear canals) for the same subject as in Fig. 2. As seen in the plot, the dual pivot model
118 introduces some bias into the trajectory of point O. In contrast, the rolling pair model is an
119 unbiased model. The average error of the rolling pair model is approximately half of that of
120 the dual pivot model (1.00 vs 1.95 cm).

121 **4. Discussion**

122 The proposed model is an extension of the analysis of movements based on the IHA.
123 Studies on the IHA have shown their potential in clinical applications but they have not
124 been oriented to modeling motion, since the IHA does not by itself convey information
125 about body position. However, the combination of the fixed and moving axodes (centrodes
126 in planar movement) gathers the kinematic information needed to reproduce the position
127 and velocities of moving bodies in any configuration.

128 The results show a good adjustment of both position and velocities variables, better
129 than provided by the dual pivot model, a representation of the neck by two revolute pairs
130 which is widely used in kinematic and dynamic applications (Woltring et al., 1994;
131 Willinger et al., 2005).

132 The rolling pair approach has previously been used for designing knee prostheses
133 (Freudenstein and Woo, 1969, Hobson and Torfason, 1975). Our method extends this
134 concept to model planar motions of complex joints under the hypothesis of a single fDOF.

135 The condition of planar motion has been verified in many studies of joint kinematics
136 based on IHA (Woltring et al., 1994, Page et al., 2009). Regarding the restriction of one

137 fDOF, there are several examples of movements of complex joints that exhibit only one
138 fDOF (Leardini et al., 1999; Page et al., 2008; Page et al., 2010). In this paper we have
139 verified that these hypotheses also apply to the flexion-extension neck movement.

140 In any case, both conditions are implicitly accepted in all models that represent
141 human joints with revolute pairs. The proposed model does not introduce any additional
142 restrictions but, on the contrary, accounts for nonfixed axes of rotation, and therefore can
143 improve current models based on revolute pairs in those cases where the actual ICR moves
144 over the range of movement.

145 Although the rolling pair does not provide detailed information about the motion of
146 internal structures, it is possible to extract some information about the nature of the
147 movement from the shape of the centrodes. For instance, the inverted U shape of the fixed
148 axode (present for all measured subjects) suggests a sequential movement of the vertebrae
149 starting with the higher vertebrae at the neutral position and following with the lower
150 vertebrae at the positions of maximum extension and flexion. This fact is illustrated in Fig.
151 4 and it has been previously observed in lumbar flexion-extension (Page et al., 2009a).

152 The estimation of IHA (or ICR) location is very sensitive to soft tissue artifacts.
153 Therefore, this model is useful in those cases in which artifacts are negligible or can be
154 efficiently controlled, e.g. neck flexion-extension (Woltring et al., 1994), lumbar flexion-
155 extension (Page et al., 2009a) or shoulder abduction-adduction (Page et al., 2010). Its
156 application to knee or ankle joints will perhaps need kinematic data from in-vitro
157 experiments (Leardini, et al., 1999; Wolf and Degani, 2007) or the use of other
158 experimental techniques that can provide a good estimation of bone motion, e.g.
159 intracortical pins or fluoroscopy (Dennis et al., 2005).

160 **Conflict of interest statement**

161 The authors have no conflicts of interest related to this work.

162 **Acknowledgement**

163 This work was funded by the Spanish Government and co-financed by EU FEDER
164 funds (Grants DPI2006-14722-C02-01, DPI2006-14722-C02-02, DPI2009-13830-C02-01,
165 DPI2009-13830-C02-02, and Ramón y Cajal contract to JAG).

166 **References**

- 167 Baydal-Bertomeu, J., García-Mas, M., Poveda, R., Belda, J., Garrido-Jaén, D., Vivas, M.J.
168 et al., 2007. Determination of simulation patterns of cervical pain from kinematical
169 parameters of movement. In: Eizmendi, G., Azkoitia, J., Craddock, G. (Eds.), *Challenges*
170 *for assistive technology, AAATE 07*, IOS Press, Amsterdam, pp. 429–433.
- 171 Dennis, D., Mahfouz, M.R., Komistek, R.D., Hoff, W., 2005. In vivo determination of
172 normal and anterior cruciate ligament-deficient knee kinematics. *Journal of*
173 *Biomechanics*, 38, 241-253.
- 174 de Zee, M., Hansen, L., Wong, C., Rasmussen, J., Simonsen, E. B., 2007. A generic
175 detailed rigid-body lumbar spine model. *Journal of Biomechanics* 40, 1219-1227.
- 176 Freudenstein, F., Woo, L., 1969. Kinematics of the human knee joint. *Bulletin of*
177 *Mathematical Biology* 2, 215-232.
- 178 Goossens, R.H.M., Snijders, C.J., 1995. Design criteria for the reduction of shear forces in
179 beds and seats. *Journal of Biomechanics* 28, 225–230.
- 180 Grip, H., Sundelin, G., Gerdle, B., Stefan Karlsson, J., 2008. Cervical helical axis
181 characteristics and its center of rotation during active head and upper arm movements—
182 comparisons of whiplash-associated disorders, non-specific neck pain and asymptomatic
183 individuals. *Journal of Biomechanics* 13, 2799-2805.
- 184 Himmetoglu, S., Acar, M., Taylor, A. J., Bouazza-Marouf, K., 2007. A multi-body head-
185 and-neck model for simulation of rear impact in cars. *Proceedings of the Institution of*
186 *Mechanical Engineers, Part D: Journal of Automobile Engineering* 221, 527-541.
- 187 Hobson DA, Torfason LE., 1975. Computer optimization of polycentric prosthetic knee
188 mechanisms. *Bulletin of Prosthetics Research* 10, 187–201.

189 Leardini, A., O'Connor, J. J., Catani, F., Giannini, S., 1999. Kinematics of the human ankle
190 complex in passive flexion; a single degree of freedom system. *Journal of Biomechanics*
191 2, 111-118.

192 Li, Z., 2006. Functional degrees of freedom. *Motor Control* 4, 301-310.

193 Page, A., Galvez, J. A., Baydal-Bertomeu, J. M., Mata, V., Belda-Lois, J. M., 2008.
194 Functional degrees of freedom of neck movements: linear models may overestimate
195 variability. *Gait & Posture Supplement* 2, S56-S56.

196 Page, A., de Rosario, H., Mata, V., Porcar, R., Solaz, J., Such, M. J., 2009a. Kinematics of
197 the trunk in sitting posture: An analysis based on the instantaneous axis of rotation.
198 *Ergonomics* 6, 695-706.

199 Page, A., de Rosario, H., Mata, V., Atienza, C., 2009b. Experimental analysis of rigid body
200 motion. A vector method to determine finite and infinitesimal displacements from point
201 coordinates. *Journal of Mechanical Design* 131, 031005 (8 pp.)

202 Page, A., Galvez, J. A., de Rosario, H., Mata, V., Prat, J., 2010. Optimal average path of the
203 instantaneous helical axis in planar motions with one functional degree of freedom.
204 *Journal of Biomechanics* 2, 375-378.

205 Petuskey, K., Bagley, A., Abdala, E., James, M. A., Rab, G., 2007. Upper extremity
206 kinematics during functional activities: Three-dimensional studies in a normal pediatric
207 population. *Gait & Posture*, 25:573-579.

208 Reuleaux, F., 1897. The kinematics of machinery. *Outlines of a Theory of Machines*.
209 MacMillan and Co., London, pp. 60-65.

210 Van der Helm, F. C. T., Veeger, H. E. J., Pronk, G. M., Van der Woude. L. H. V.,
211 Rozendal, R. H., 1992. Geometry parameters for musculoskeletal modelling of the
212 shoulder mechanism. *Journal of Biomechanics* 25, 129-144.

213 Willinger, R., Bourdet, N., Fischer, R., Le Gall, F., 2005. Modal analysis of the human neck
214 in vivo as a criterion for crash test dummy evaluation. *Journal of Sound and Vibration*
215 287: 405-431

216 Wolf, A., Degani, A., 2007. Recognizing knee pathologies by classifying instantaneous
217 screws of the six degrees-of-freedom knee motion. *Medical and Biological Engineering*
218 *and Computing* 5, 475-482.

219 Woltring, H. J., Long, K., Osterbauer, P. J., Fuhr, A. W., 1994. Instantaneous helical axis
220 estimation from 3-D video data in neck kinematics for whiplash diagnostics. *Journal of*
221 *Biomechanics* 12, 1415-1432.

1 **FIGURE LEGENDS**

2 Fig. 1. a) The position of the distal body with respect to a reference position is given by
3 the joint angle θ and the displacement of a given point G , $\Delta\mathbf{R}_G(\theta)$. Infinitesimal
4 displacements are described by means of angular and linear velocities, \mathbf{w} and \mathbf{v}_G ,
5 respectively. b) The fixed centrode is the curve described by point H , H_0H . It depends
6 on the instantaneous variables. We can obtain the moving centrode at the reference
7 position, H_0H_1 , by applying the finite displacement $-\{\theta ; \Delta\mathbf{R}_G\}$ to the distal segment.
8 Then point H moves to H_1 .

9

10

11 Fig. 2. Centroides of the neck flexion-extension movement of a subject, represented at
12 the neutral position ($\theta=0^\circ$). The fixed centrode is plotted as the solid black curve; the
13 moving centrode is the dotted black curve. As the head moves from the neutral position,
14 the moving axode rolls without slipping over the fixed axode. The skull and spinal
15 structures are figurative representations (no radiographs were taken), based on the
16 locations of the anatomical markers.

17

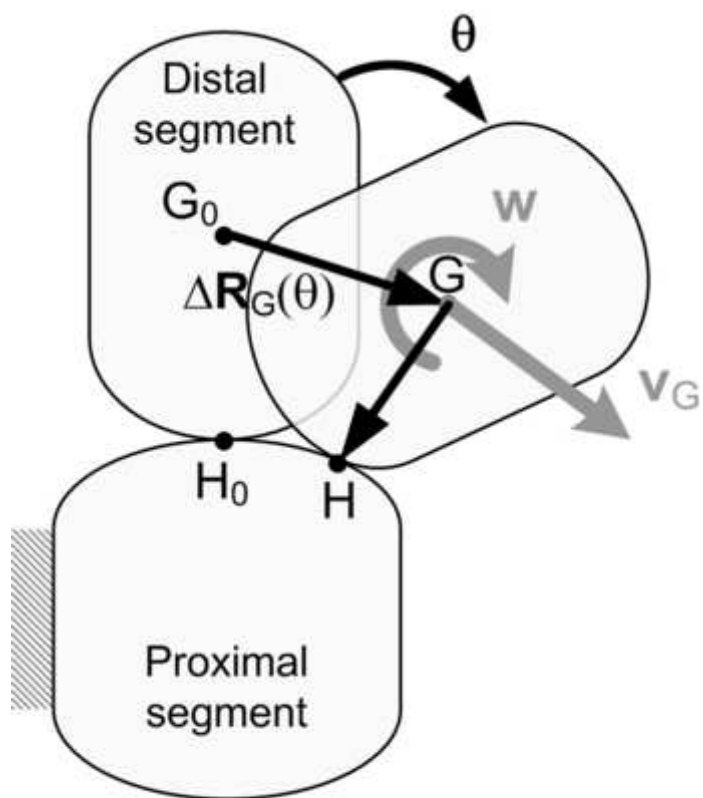
18

19 Fig. 3. Measured and estimated path of anatomical point O (the midpoint of markers
20 located at the ears). The rolling pair model (grey solid line) provides an unbiased
21 estimation of the mean path, corresponding to the averaged trajectory obtained in the
22 process of averaging across cycles. In contrast, the dual pivot model assumes a fixed
23 axis of rotation at $C7-T1$ level, therefore the length of $C7-O$ is constant. This introduces
24 a bias in the estimation of the path of point O and increases the RMS error.

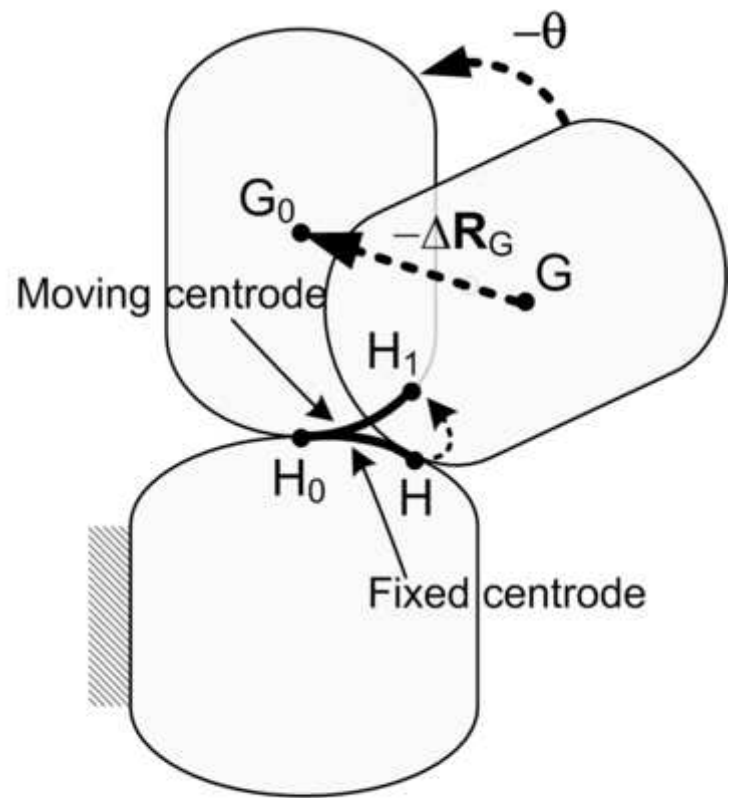
25

26 Fig. 4. Interpretation of the sequential movement of vertebrae from the shape of the
27 centrodes. The motion of the head relative to the thorax can be decomposed into a set of
28 small angular displacements of each vertebra with regard to the one below, the axes of
29 which are approximately on the intervertebral discs. In the picture, we represent these
30 angular vectors as circles with their radius proportional to the magnitude of the angle.
31 The measured global motion is the sum of all intervertebral rotations, with a global ICR
32 located at the centroid of that system (Page et al, 2009a). (a) In the neutral position the
33 ICR is located at the top of the fixed centrode, H_N , near C1; therefore the global motion
34 at this position is mainly caused by the contribution of the upper vertebrae. (b) As the
35 neck flexes, the ICR moves down on the fixed axode to H_F ; this implies a downwards
36 sequential motion of vertebrae. The skull and spinal structures are figurative
37 representations (no radiographs were made), based on the locations of the anatomical
38 markers.

Figure 1
[Click here to download high resolution image](#)



(a)



(b)

Figure2
[Click here to download high resolution image](#)

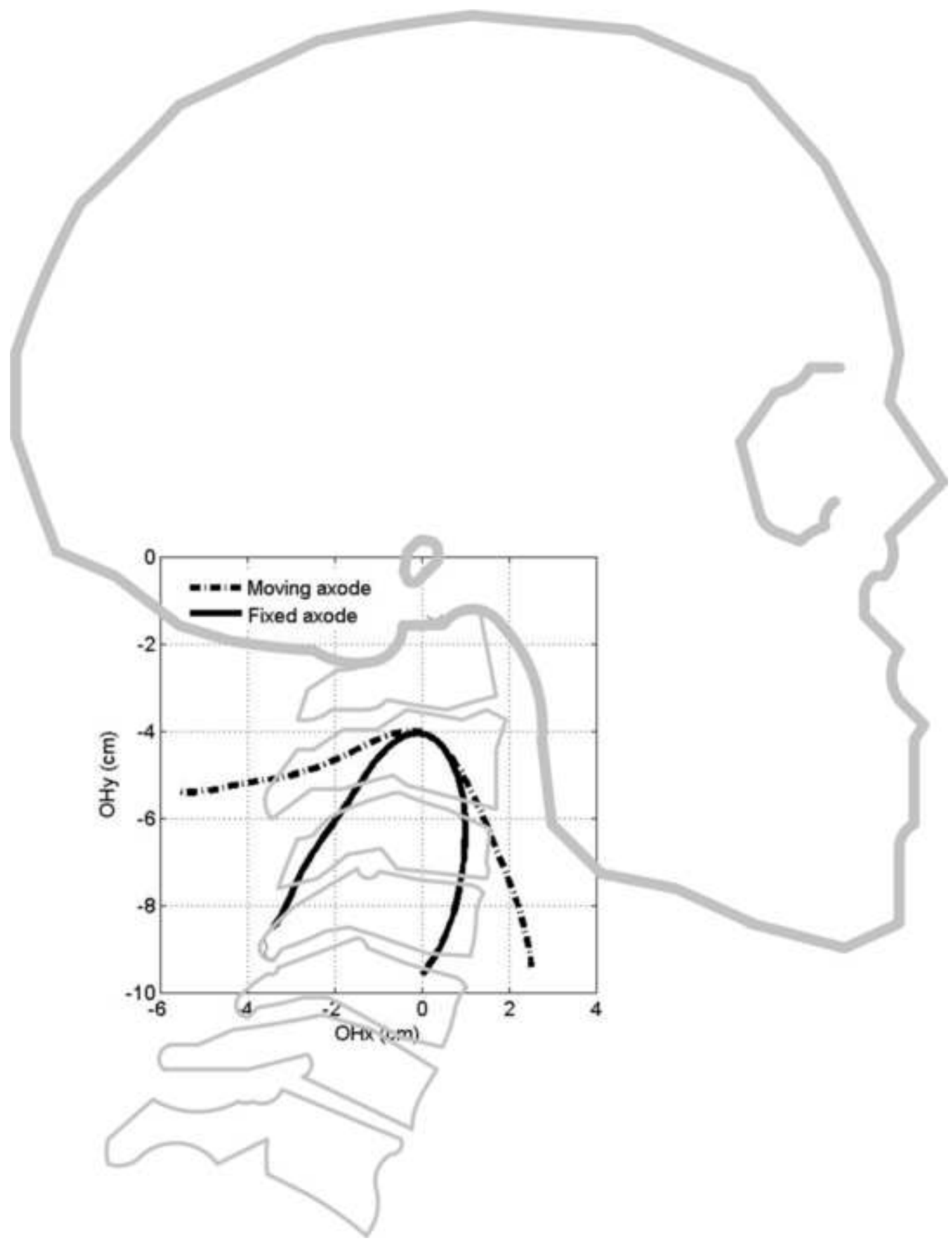


Figure3
[Click here to download high resolution image](#)

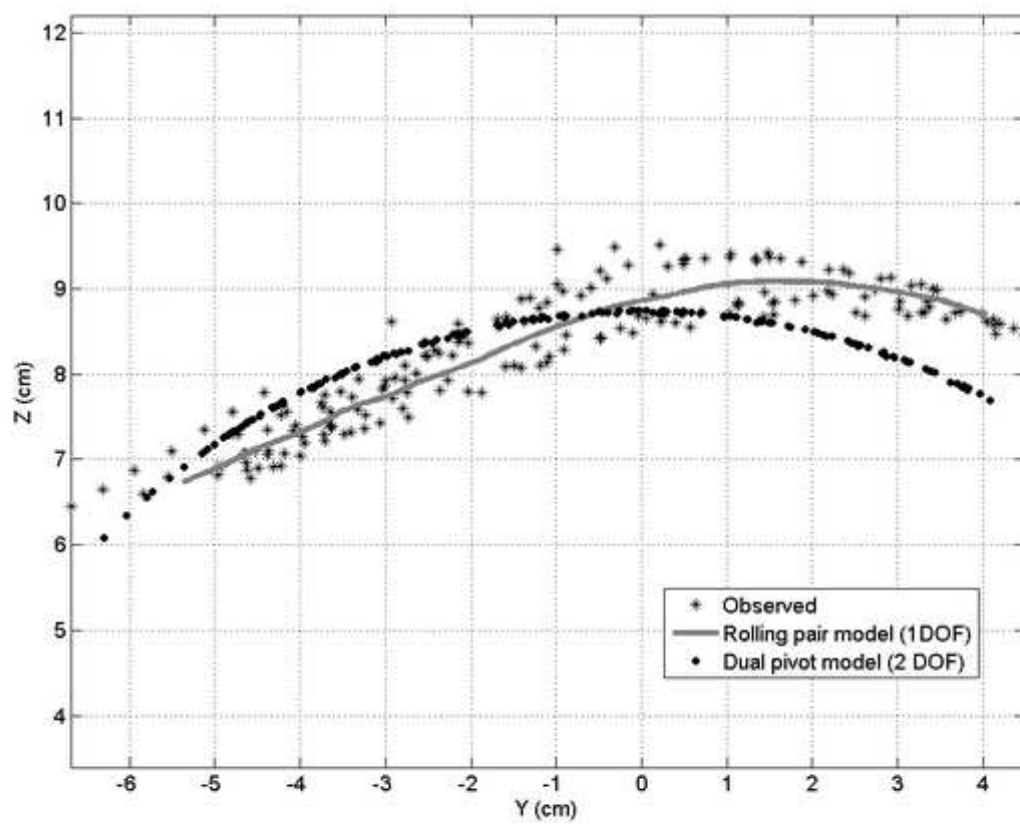


Figure4
[Click here to download high resolution image](#)

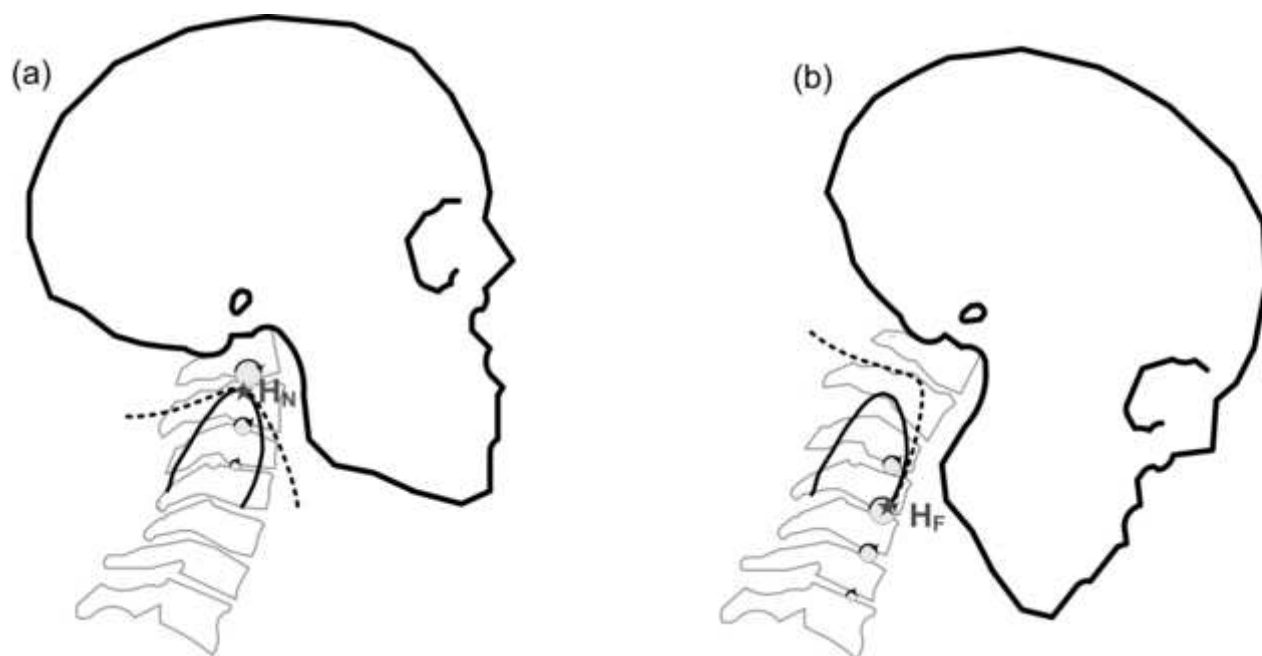


Table 1

Verification of the hypotheses of one functional degree of freedom (fDOF) and planar movement. Comparison between rolling pair and dual pivot model.

Variable	Description	Mean (n=12)	SD (n=12)
R _{pos}	Multiple correlation coefficient between measured and fitted coordinates of point G	0.995	0.005
R _{vel}	Multiple correlation coefficient between measured and fitted values of v_G	0.958	0.025
p95 (α)	Percentile 95 of the angle between the average direction perpendicular to motion, \mathbf{u} , and the measured $\mathbf{w}(t)$, for each subject ($^\circ$)	3.9	1.0
p95(β)	Percentile 95 of the deviation from 90° of the angle between linear velocity, v_G , and angular velocity, $\mathbf{w}(t)$, for each subject ($^\circ$)	2.1	0.8
Error RP	RMS error of the distance between measured positions of point O and those estimated by the rolling-pair model (cm).	1.00	0.28
Error DP	RMS error of the distance between measured positions of point O and those estimated by the dual pivot model (cm)	1.95	1.00